Role of Transthoracic Echocardiography in Early Diagnosis of Williams Syndrome in the Neonatal Period

Kazuhiro Nomura, BHS, Takahisa Moronuki, AS, Shinichi Takeuchi, AS, Takuya Maeda, MD, PhD, Koichi Toda, MD, and Toshiki Kobayashi, MD, *Saitama, Japan*

INTRODUCTION

Williams syndrome (WS) is a multisystem disorder characterized by growth abnormalities with facial abnormalities, numerous endocrine and connective tissue disorders, and cardiovascular disease (CVD), including supravalvular aortic stenosis (SVAS) and peripheral pulmonary stenosis (PPS). Williams syndrome results from de novo deletion of approximately 1.55 to 1.83 Mb on chromosome 7q11.23 and occurs in about 1 in 10,000 live births. Williams syndrome is usually suspected based on its characteristic facial features, but it is often unrecognized during the neonatal period, and complications may progress prior to diagnosis.[1] Moreover, the naturally progressive clinical courses of SVAS and PPS are variable, and the timing of surgery or intervention for these cardiac complications of WS depends on the progression of vascular stenosis. In fact, SVAS has been reported to occur in 45% to 75% of patients with WS and PPS in about 40%.[2]

This report describes a patient who developed SVAS and PPS at 26 days of age before diagnosis of WS and in whom SVAS progressed rapidly over 16 days. This case highlights the importance of short-term follow-up by transthoracic echocardiography (TTE) in neonates with SVAS and PPS and of keeping in mind the possibility of WS.

CASE PRESENTATION

A 37-year-old woman who had had a previous miscarriage was admitted to our hospital at 31 weeks and 1 day of gestation with fetal growth arrest after being diagnosed with umbilical cord torsion at 24 weeks and 1 day of gestation. Induction of labor was scheduled at 37 weeks and 3 days but there were frequent severe late decelerations, leading to delivery by emergency cesarean section. A female infant with a weight of 1,819 g, length of 42.6 cm, and Apgar scores of 8 and 9 was born at a gestational age of 37 weeks and 3 days. At birth (day 0), the patient had a pulse rate of 156 beats per minute, blood pressure of 72/28 mm Hg, and oxygen saturation of 97% on room air. Unexplained fetal growth retardation was evident, but serology ruled out TORCH syndrome (a group of newborn infections including toxoplasmosis, other agents, rubella, cytomegalovirus, and herpes simplex) and inborn errors of metabolism.

Screening TTE performed on day 0 showed a left ventricular ejection fraction (LVEF; Teichholz method) of 72%, normal left ventricular wall motion, a patent foramen ovale, and a patent ductus arteriosus with a diameter of 1.8 mm. On day 26, a follow-up TTE performed after a heart murmur was heard showed an LVEF of 74%, an interventricular septal thickness of 3.0 mm (*Z* score, −0.77), a left ventricular posterior wall thickness of 3.0 mm (*Z* score, 0.47), a left ventricular end-diastolic diameter of 16.8 mm (*Z* score, −0.29), and a left ventricular end-systolic diameter of 10.1 mm (*Z* score, −0.46; Video 1). There was no left ventricular hypertrophy (LVH) or patent ductus arteriosus. Transthoracic echocardiography with color Doppler showed mild aortic regurgitation and mosaic signals from the superior border of the sinus of Valsalva to the descending aorta (Figure 1A, Video 2), right pulmonary artery (RPA), and left pulmonary artery (LPA; Figure 1B, Video 3). Therefore, the descending aorta, main pulmonary artery, RPA, and LPA were observed in more detail from the superior border of the sinus of Valsalva, which was found to be markedly thickened, and the lumen of the vessel was narrowed to 2.2 mm in diameter (*Z* score, −8.72), indicating hourglass-type SVAS (Figure 2A). The ascending aorta (diameter, 4.1 mm), transverse arch (diameter, 3.8 mm; *Z* score, −4.21), and distal arch (diameter, 3.9 mm; *Z* score, −2.18) were open. The aortic isthmus was observed to be slightly narrower at 2.8 mm in diameter (*Z* score, −3.66), but the flow velocity at the site of anastomosis in the ascending aorta was 2.94 m/sec (Figure 2B). The main pulmonary artery was 4.4 mm in diameter (*Z* score, −3.53) with an open vessel lumen, but the lumens of the RPA (diameter, 2.1 mm; *Z* score, −4.42) and LPA (diameter, 3.4 mm; *Z* score, −1.09) were narrowed, indicating bilateral PPS (Figure 3A). The flow velocity was 3.61 m/sec in the RPA and 2.90 m/sec in the LPA (Figure 3B). Transthoracic echocardiography revealed that the origins of the right coronary artery, left main coronary trunk, left anterior descending artery, and left circumflex artery were all consistently normal at each observation time point. The characteristic facial features of WS, including a narrow interorbital space, saddle nose, and plump cheeks, were more pronounced on day 42 than on day 26. A diagnosis of WS was finally confirmed by chromosomal analysis, which found a 7q11.23 microdeletion.

On day 42, TTE showed moderate aortic regurgitation (Figure 4A) but more rapid progression of SVAS than on day 26 and a flow velocity of 4.11 m/sec (Figure 4B). The diameter of the aorta was 3.4 mm (*Z* score, −5.80) at the superior border of the sinus of Valsalva, 4.6 mm (*Z* score, −3.26) at the transverse arch, 2.7 mm (*Z* score, −4.14) at the aortic isthmus, and 3.3 mm (*Z* score, −3.46) at the distal arch. The diameter of the pulmonary artery was 2.2 mm (*Z* score, −4.48) at

From the Department of Laboratory Medicine, Saitama Medical University Hospital (K.N., T.M., S.T., T.M.); and Department of Pediatric Cardiology, Saitama Medical University International Medical Center (K.T., T.K.), Saitama, Japan.

Keywords: Williams syndrome, Supravalvular aortic stenosis, Peripheral pulmonary artery stenosis, Transthoracic echocardiography

Conflicts of interest: The authors reported no actual or potential conflicts of interest relative to this document.

Correspondence: Kazuhiro Nomura, BHS, Department of Laboratory Medicine, Saitama Medical University Hospital, 38 Morohongo, Moroyama-Machi, Iruma-gun, Saitama 350-0495, Japan. (E-mail: *k_nomura@saitama-med.ac.jp*).

Copyright 2022 by the American Society of Echocardiography. Published by Elsevier Inc. This is an open access article under the CC BY-NC-ND license (http://creativecommons.org/licenses/by-nc-nd/4.0/).

2468-6441

https://doi.org/10.1016/j.case.2022.08.006

VIDEO HIGHLIGHTS

Video 1: Two-dimensional TTE, parasternal long-axis view, day 26, demonstrates the SVAS (and nonstenotic aortic valve). *LA*, Left atrium; *LV*, left ventricle; *RV*, right ventricle.

Video 2: Two-dimensional TTE, parasternal long-axis view with color Doppler demonstrates turbulent flow at the superior border of the sinus of Valsalva and the RPA branch behind the LA. *LA*, Left atrium; *LV*, left ventricle; *RV*, right ventricle.

Video 3: Two-dimensional TTE, basal parasternal short-axis view with color Doppler demonstrates turbulent flow in the RPA and LPA branches. *MPA*, Main pulmonary artery.

Video 4: Two-dimensional TTE, parasternal long-axis view performed before surgery demonstrates significant interval LV wall thickening. *LA*, Left atrium; *RV*, right ventricle.

View the video content online at www.cvcasejournal.com.

the RPA and 3.0 mm (*Z* score, −2.13) at the LPA. Cardiac computed tomography (CCT) was performed to evaluate the morphology of the SVAS (Figure 5) and PPS (Figure 6) and yielded results comparable with those of TTE. Cardiac computed tomography also did not detect arterial stenosis in the right coronary artery, left main coronary trunk, left anterior descending artery, or left circumflex artery. Preoperative TTE showed an LVEF of 81%, an interventricular septal thickness of 9.7 mm (*Z* score, 4.19), a left ventricular posterior wall thickness of 9.0 mm (*Z* score, 5.36), a left ventricular end-diastolic diameter of 18.8 mm (*Z* score, −1.46), and a left ventricular end-systolic diameter of 10.0 mm (*Z* score, −2.34) with clear LVH (Video 4). The flow velocity in the ascending aorta was 5.63 m/sec, indicating very severe SVAS (Figure 7). On day 132 after birth, when the patient weighed 5,500 g, the SVAS was repaired using the 3-patch method with reconstruction using a bovine pericardial patch.

Postoperative TTE at about 1 month after surgery showed that the flow velocity was 1.44 m/sec at the site of anastomosis in the ascending aorta. The flow velocity was 3.46 m/sec in the RPA and 2.87 m/sec in the LPA. The SVAS and PPS were evaluated on CCT at the same time after surgery (Figure 8). The SVAS showed a decrease in flow velocity from the preoperative value and no worsening of LVH was observed. However, there was no change in the PPS from the preoperative state in terms of blood flow velocity or morphology.

DISCUSSION

The prognosis of SVAS associated with WS remains controversial. Supravalvular aortic stenosis is the most critical and frequent

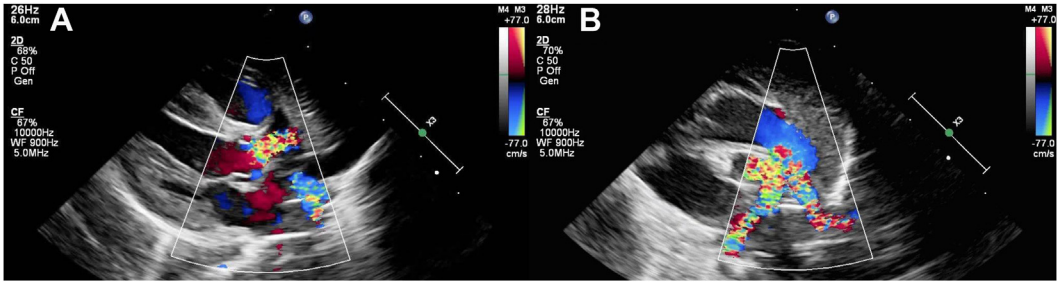

Figure 1 Two-dimensional TTE with color Doppler images obtained at day 26. **(A)** Parasternal long-axis view, systolic phase, demonstrates turbulent flow pattern in the ascending aorta. **(B)** Parasternal short-axis view at the base, systolic phase, demonstrates turbulent flow in both the right and left pulmonary arteries.

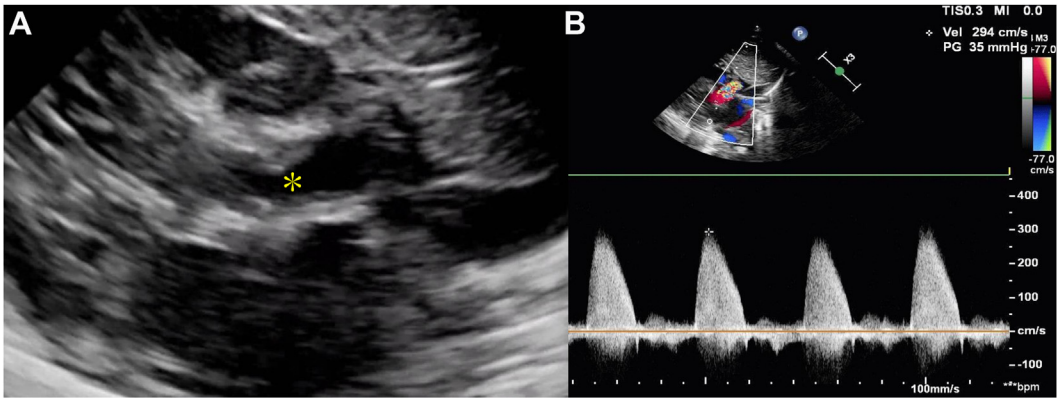

Figure 2 **(A)** Two-dimensional TTE, parasternal long-axis view, systolic phase, demonstrates the superior border of the sinus of Valsalva is markedly thickened and the lumen of the ascending aorta is narrowed (*asterisk*). **(B)** Two-dimensional TTE, suprasternal notch view with color-guided continuous-wave spectral Doppler interrogation demonstrates a high-velocity 2.94 m/sec jet corresponding to a peak gradient of 35 mm Hg.

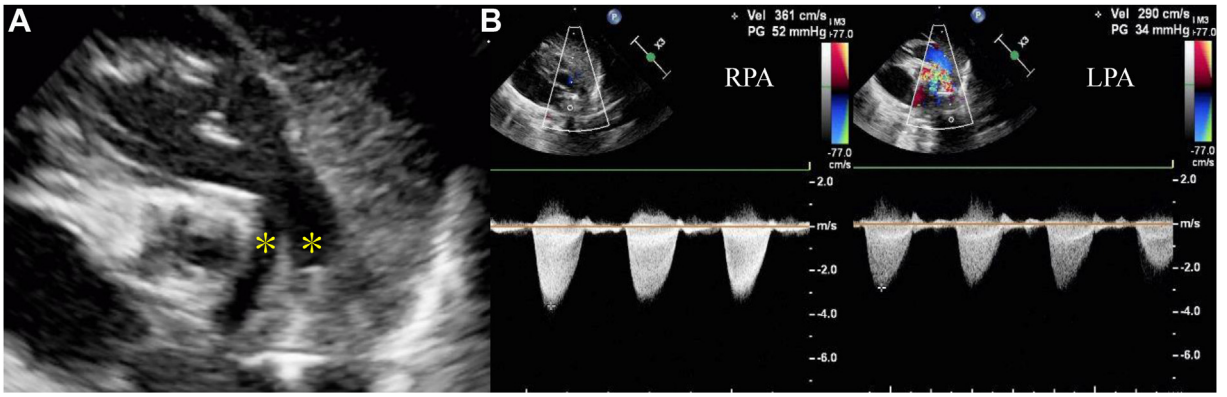

Figure 3 Two-dimensional TTE, parasternal short-axis view at the base, systolic phase, demonstrates **(A)** patent main pulmonary artery and luminal narrowing in the right and LPA branches (*asterisks*). **(B)** Color-guided continuous-wave spectral Doppler interrogation confirms high-velocity of 3.61 m/sec in the RPA (*left panel*) and 2.90 m/sec in the LPA (*right panel*) corresponding to peak gradients of 52 mm Hg and 34 mm Hg, respectively.

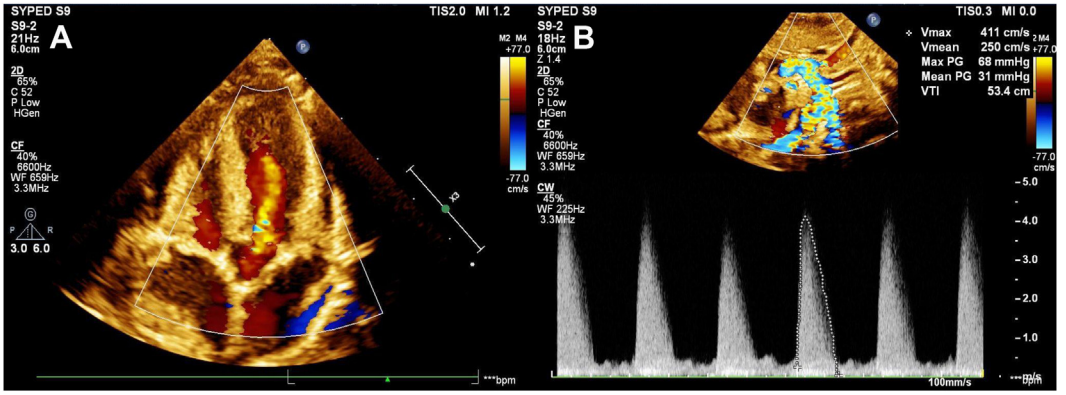

Figure 4 **(A)** Two-dimensional TTE, apical 5-chamber view with color Doppler, diastolic phase, demonstrates moderate aortic valve regurgitation. **(B)** Two-dimensional TTE, suprasternal notch view with color-guided continuous-wave spectral Doppler interrogation confirms a high-velocity jet of 4.11 m/sec corresponding to a peak gradient of 68 mm Hg.

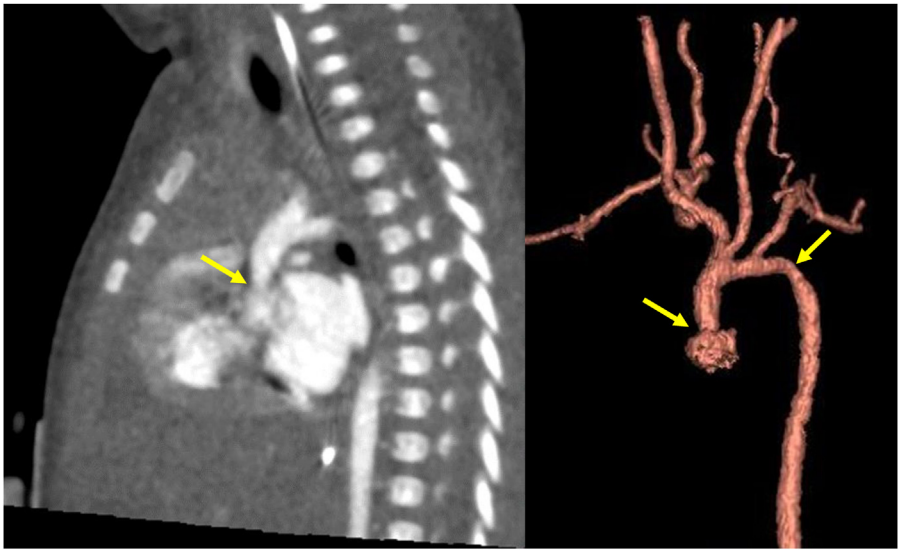

Figure 5 Contrast-enhanced CCT, sagittal display (*left panel*) and volume-rendered 3D cropped view (*right panel*) obtained at 1 month after birth demonstrates hypoplasia of the sinotubular junction and aortic isthmus (*arrows*).

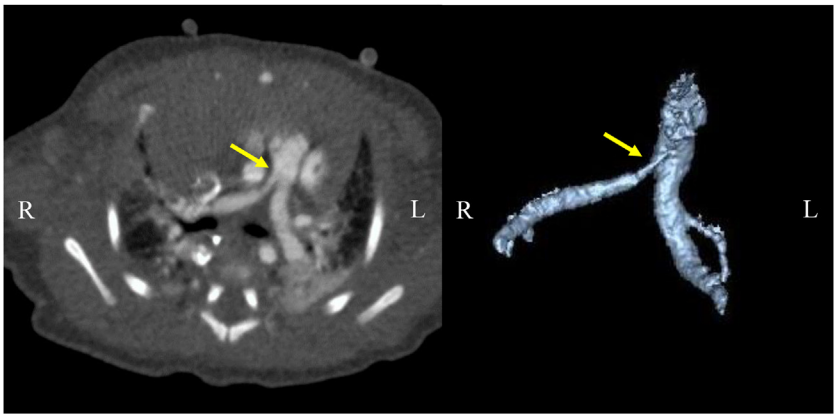

Figure 6 Contrast-enhanced CCT, axial display (*left panel*) and volume-rendered 3D cropped view (*right panel*) obtained at 1 month after birth demonstrates PPS that involves the RPA to the greatest degree (*arrows*).

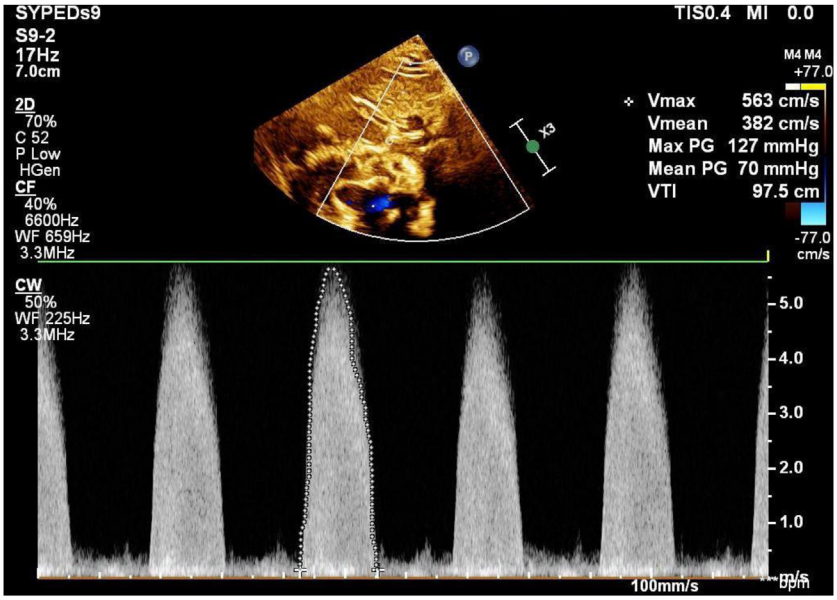

Figure 7 Two-dimensional TTE, suprasternal notch view with color-guided continuous-wave spectral Doppler interrogation of the ascending aorta confirms a high-velocity jet of 5.63 m/sec corresponding to a peak gradient of 127 mm Hg.

cardiovascular abnormality in infants with WS and has been reported to be progressive, especially during the first 5 years of life, whereas PPS is the second most common cardiovascular abnormality and reportedly improves spontaneously.[3,4] As mentioned above, SVAS is often found to be progressive in patients with WS. However, Collins *et al*[2] reported findings that were not consistent with those in most of the literature.[1,5-7] Specifically, they found that stenosis may progress in patients with WS and moderate to severe SVAS at birth but remains stable in the majority of mild complications.[2] According to another report by Collins *et al*,[8] WS-associated SVAS progressed in only 10% of cases. In our case, both SVAS and PPS developed after birth and before the age of 26 days. Moreover, the SVAS progressed rapidly in the following 16 days, whereas there was no change in the PPS in terms of blood flow velocity or morphology after diagnosis. Transthoracic echocardiography is suitable for short-term and noninvasive follow-up of CVD, whereas CCT, which is suitable for precise and detailed evaluation of CVD, cannot be performed repeatedly in a short period of time since it exposes the patient to radiation and requires contrast administration. The rapid progression of SVAS 16 days after diagnosis in the present case highlights the critical role that TTE can play in the early diagnosis of WS.

Individuals with both SVAS and PPS may develop biventricular hypertrophy and hypertension, which increases the risk of myocardial ischemia, dysrhythmia, and sudden death.[9] Coronary abnormalities are also often associated with congenital SVAS.[10] Bird *et al*[11] previously reported that the pathology of 7 autopsy cases suggested 2 anatomic abnormalities that predispose patients with WS to sudden death: coronary stenosis and severe biventricular outflow tract obstruction. The mechanisms of sudden death included myocardial ischemia, decreased cardiac output, and arrhythmia. Therefore, continuous monitoring of these findings with TTE will enable proactive identification of patients at high risk of sudden death. However, WS should be differentiated

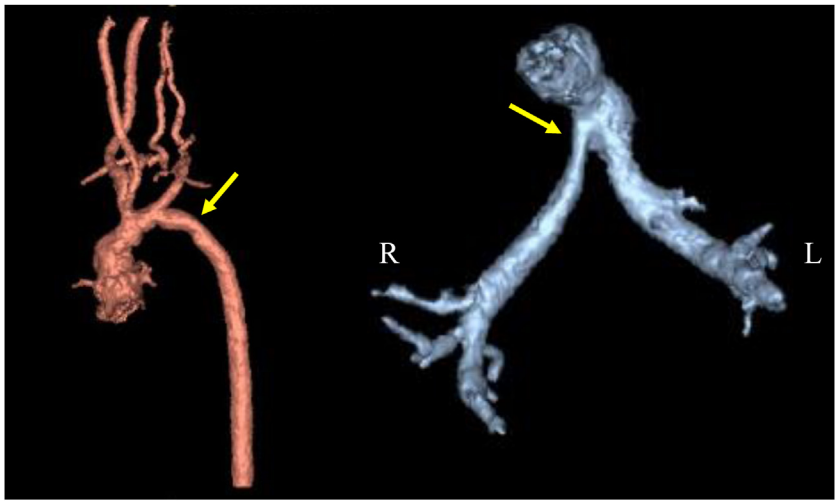

Figure 8 Contrast-enhanced CCT, volume-rendered 3D cropped views obtained 1 month after surgery demonstrates hypoplasia (*arrows*) of the aortic isthmus (*left panel*) and PPS (*right panel*).

from other syndromes that are characterized by developmental delay, attention-deficit hyperactivity disorder, short stature, distinctive facies, and congenital heart disease.[12] It has been reported to be difficult to detect these characteristics and abnormalities in newborns.[1] Therefore, if a patient is diagnosed with SVAS and PPS, TTE should be performed and repeated in a short period of time to carefully track the progression of both stenoses, keeping in mind the possibility of WS.

CONCLUSION

Supravalvular aortic stenosis coexisting with WS has the potential to develop rapidly. Although the surgical treatment for SVAS is still controversial, an extended 3-patch SVAS repair is likely to be the best option. It is often difficult to diagnose WS based on the characteristic facial appearance in the neonatal period. Transthoracic echocardiography can play an important role in the diagnosis and evaluation of major cardiac abnormalities noted in patients with WS.

SUPPLEMENTARY DATA

Supplementary data related to this article can be found at https://doi.org/10.1016/j.case.2022.08.006.

REFERENCES

1. Eronen M, Peippo M, Hiippala A, Raatikka M, Arvio M, Johansson R, et al. Cardiovascular manifestations in 75 patients with Williams syndrome. J Med Genet 2002;39:554-8.
2. Collins TR II. Cardiovascular disease in Williams syndrome. Circulation 2013;127:2125-34.
3. Pober BR, Johnson M, Urban Z. Mechanisms and treatment of cardiovascular disease in Williams-Beuren syndrome. J Clin Invest 2008;118:1606-15.
4. Collins TR II, Kaplan P, Somes GW, Rome JJ. Long-term outcomes of patients with cardiovascular abnormalities and Williams syndrome. Am J Cardiol 2010;105:P874-8.
5. Giddins NG, Finley JP, Nanton MA, Roy DL. The natural course of supravalvar aortic stenosis and peripheral pulmonary artery stenosis in Williams's syndrome. Br Heart J 1989;62:315-9.
6. Kececioglu D, Kotthoff S, Vogt J. Williams-Beuren syndrome: a 30-year follow-up of natural and postoperative course. Eur Heart J 1993;14:1458-64.
7. Kim YM, Yoo SJ, Choi JY, Kim SH, Bae EJ, Lee YT. Natural course of supravalvar aortic stenosis and peripheral pulmonary arterial stenosis in Williams' syndrome. Cardiol Young 1999;9:37-41.
8. Collins TR II, Kaplan P, Somes GW, Rome JJ. Cardiovascular abnormalities, interventions, and long-term outcomes in infantile Williams syndrome. J Pediatr 2010;156:253-8.
9. Pham PP, Moller JH, Hills C, Larson V, Pyles L. Cardiac catheterization and operative outcomes from a multicenter consortium for children with Williams syndrome. Pediatr Cardiol 2009;30:9-14.
10. Yilmaz AT, Arslan M, Ozal E, Býngöl H, Tatar H, Oztürk OY. Coronary artery aneurysm associated with adult supravalvular aortic stenosis. Ann Thorac Surg 1996;62:1205-7.
11. Bird LM, Billman GF, Lacro RV, Spicer RL, Jariwala LK, Hoyme HE, et al. Sudden death in Williams syndrome: report of ten cases. J Pediatr 1996;129:926-31.
12. Morris CA. Williams syndrome. In: Adam MP, Ardinger HH, Pagon RA, et al., editors. GeneReviews [Internet]. Seattle: Washington University Press; 1993-2022:1-30.